inter·noise 2023
CHIBA,GREATER TOKYO 20-23 AUGUST

# Evaluation test of circular acoustic reflector based on number theory prototyped made utilizing additive manufacturing

Yoshinori Takahashi[1]
Kogakuin University
2665-1 Nakanomachi, Hachioji-shi, Tokyo 192-0015 Japan

Isao Makino[2]
Kogakuin University
2665-1 Nakanomachi, Hachioji-shi, Tokyo 192-0015 Japan

**ABSTRACT**

*As an application of number theory to the field of acoustics, acoustic reflectors with phase diffraction grating based on Galois fields or primitive roots have been studied. These reflectors have a structure with equally spaced depressions of irregular depth that diffuse acoustic wave in various directions. To generate the sequence of irregular numbers needed to determine the depth of the concavity, methods such as using a primitive element of a Galois field the remainder of the power of a primitive root of a prime number have been proposed. In either method, the depth of the depressions is taken from* 0 *to half of the wavelength of the sound wave to be diffused, and the spacing between the protrusion or depression is designed to be quarter of the wavelength, resulting in a rectangular shaped reflector. The proposed method not only allows the design to change from rectangular to circular, but also makes it possible to construct a structure corresponding to multiple wavelengths on a single reflector. In this report, the effectiveness of the proposed reflector will be demonstrated through a model experiment of a prototyped reflector by using additive manufacturing.*

## 1. INTRODUCTION

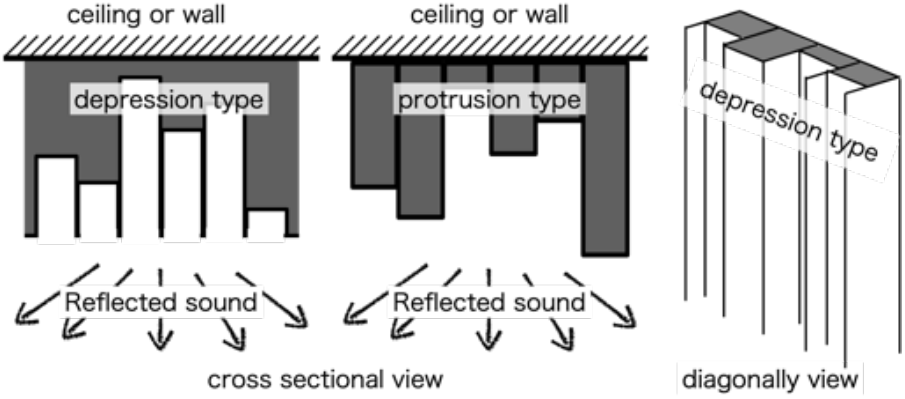


Figure 1: Example of acoustic reflector

[1]yoshinori@cc.kogakuin.ac.jp
[2]makino_i@cc.kogakuin.ac.jp

Research of concert halls has been conducted for many years, and attempts have been made to evaluate halls by focusing on the arrival direction of the reflected sound [1]. Acoustic reflectors are used in concert halls, recording studio or listening room, where various types of diffusers are designed to adjust the sound balance. When walls or ceiling have different projections of heights, the reflected waves from each projection interfere with each other and are reflected in a different direction than if they were reflected from a plane surface. The general principle of acoustic reflectors is that the creation of projections or depressions of various heights causes complex interference and diffuses reflected waves [2]. Based on this principle, acoustic reflectors has been proposed since the late 1970s to diffuse reflected sound waves in various directions by creating a random number of projections or depressions with length ranging from 0 to $1/2$ the wavelength, as shown in Fig. 1section 14.8 –14.9 of [3]).

The generation and placement of projections of various length of depressions of various depth are determined based on the number theory, such as Galois fields or primitive roots. It is possible to arrange projections or depressions in two dimensions, and it has already been put to practical use. For example, Blackbird Studio C in Nashville, Tennessee, USA is well known. In such a reflector based on number theory, the hight or depth of the projections or depressions In reflectors based on number theory, the hight or depth of the projection or depression takes values from 0 to $1/2$ of the wavelength $\lambda$ to be diffused a sound, and the spacing between the projection or depression is designed so that the distance between them is $\lambda/4$. In the two-dimensional case, "Sino-representation" based on the Chinese Remainder theorem is used, therefore the shape of the reflector becomes a rectangular (chapter 17 of [3]).

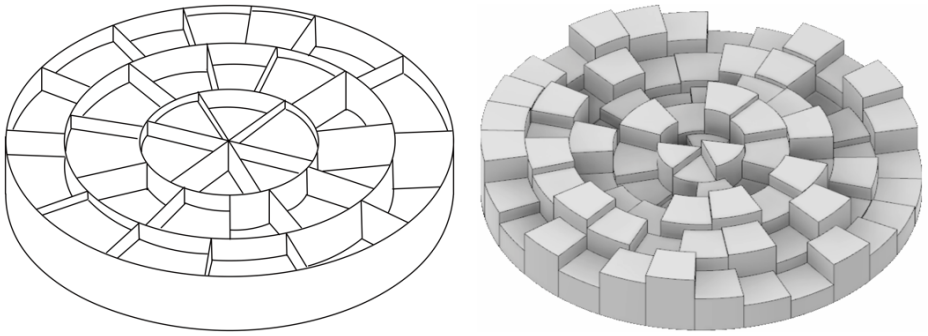

(a) (b)

Figure 2: Circular acoustic reflector which had been proposed in this paper

On the other hand, with the developing the construction technologies, rooms of various shapes, such as circular, oval and open-air atrium, etc. are being built. However, acoustic problems associated with room shapes have also been reported [4]. The installation of acoustic reflectors on walls and ceilings is considered to be one of the effective method to control the acoustic environment. In order to design reflectors that can accommodate rooms of various shapes, it is important to provide design choices. If reflectors that shapes other than rectangular can be designed while maintaining diffusion performance, it is expected to increase design selectivity. Therefore, the authors have been proposing a reflector with a circular arrangement of depressions or projections as show in Fig. 2, using an irregular number sequence based on primitive roots [5]. The proposed method is able to expand the design possibilities of the room in which it is installed by allowing the reflector design to change from a rectangular to a circular shape. Furthermore, the proposed method makes it possible to construct corresponding to multiple wavelengths on a single reflector. This report introduces the design of the proposed circular reflector. The prototyped of a reflector utilizing additive manufacturing (3D printer) and the results of an experiment using the reflector will be described.

## 2. DESIGN OF CIRCULAR REFLECTOR BASED ON PRIMITIVE ROOTS

The circular reflector proposed in this report consists of a circumferential array of projections or depressions of depth $d$ as shown in Fig. 3, using the power residue of the primitive root corresponding to a prime number. The depth $d$ is not a constant, however an irregularly selected value in the range 0 – 1/2 of the wavelength $\lambda$ of the sound wave to be diffused.

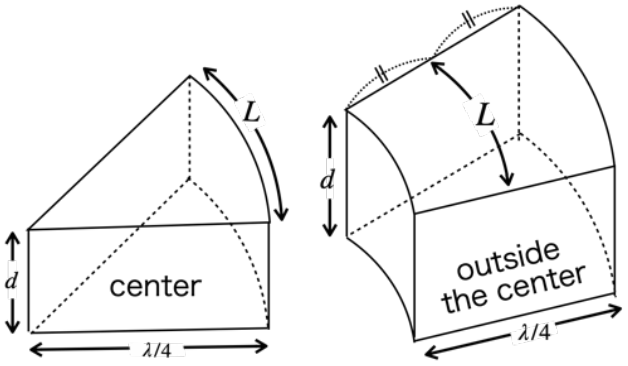


Figure 3: Structure of circular reflector

The projections or depressions are radially divided into $\lambda/4$ to be targeted, and fan-shaped projections or depressions are arranged in a ring. In this case, the circumferential projections or depressions are divided so that its length $L$ is close to $\lambda/4$. If the desired number of divisions of the $n$th ring from the center is $L_N(n)$, the inner circumference of the ring is $(n-1)2\pi\,(\lambda/4)$, the outer circumference is $n2\pi\,(\lambda/4)$, and the average of the outer circumferences is $(2n-1)\,\pi\,(\lambda/4)$.

Therefore, the ideal division of circumscription of the $n$th ring can be explane $(2n-1)\,\pi$. This value is not a natural number. The proposed method uses the primitive root of prime $p$ to make the $p-1$ division, the number of division becomes $(2n-1)\,\pi \fallingdotseq p-1$. That is, for the division of the $n$th ring from the center, the prime number $p$ closest to $(2n-1)\,\pi+1$ is used, which is close to the ideal number of divisions. However, the central piece $n=1$ is divided into 4 pieces, which makes the pieces extremely large. In this study, the center circle was divided into 6 segments so that the arc length $L$ is close to $\lambda/4$. The hight of the projections $d$ is a random sequence of integers from 1 to $p-1$ using the remainder of the power of the primitive root of $p$. By multiplying the hight by this integer sequence $\lambda/(2p)$, it can be expected the reflections to be generated in the direction $p-1$.

When small primitive roots are used for large prime, powers of the primitive roots may appear in the initial part of the remainder sequence. To prevent this problem, primitive roots should be large. For example, if 2 is select as the primitive root of $p=29$, the sequence of the reminder of the powers of the primitive root becomes 2, 4, 8, 16, 3, 6, 12, 24, 19, 9, 18, 7, 14, 28, 27, 21, 13, 26, 23, 17, 5, 10, 20, 11, 22, 15, 1. Up to the power of 4, there will always be a staircase power of 2 that remains a power of 2: 2, 4, 8, 16. The larger the prime number, the longer the length of such a section. On the other hand, if 27 is chosen as the primitive root of $p=29$, then 27, 4, 21, 16, 26, 6, 17, 24, 10, 9, 11, 7, 15, 28, 2, 25, 8, 13, 3, 23, 12, 5, 19, 20, 18, 22, 14, 1, and the powers of the primitive root will not appear as they are in the initial part of the remainder sequence.

The number of primitive roots varies with the prime number, and the number si represented by $\phi(p-1)$ using Euler's function $\phi$. There are 12 primitive roots of 2, 3, 8, 10, 11, 14, 15, 18, 19, 21, 26, 27 for $p=29$ shown as an example. Therefor, it is easy to design reflectors with different patterns of projections by changing the primitive roots. Table 2 shows prime number $p$ up to $n=3$, its largest primitive root $r$, and the remainder of power of $r$ in $p$.

Since the last ($p-1$th) of one cycle of a reminder sequence is always 1, starting form the same point to line up the projections will cause a problem of pieces of the same hight in the radial direction. Fig. 4(a) shows the arrangement the remainder in the circular reflector according to such a rule. By setting the period of the remainder sequence to $p-1$ starting from the 10th power, it is possible to

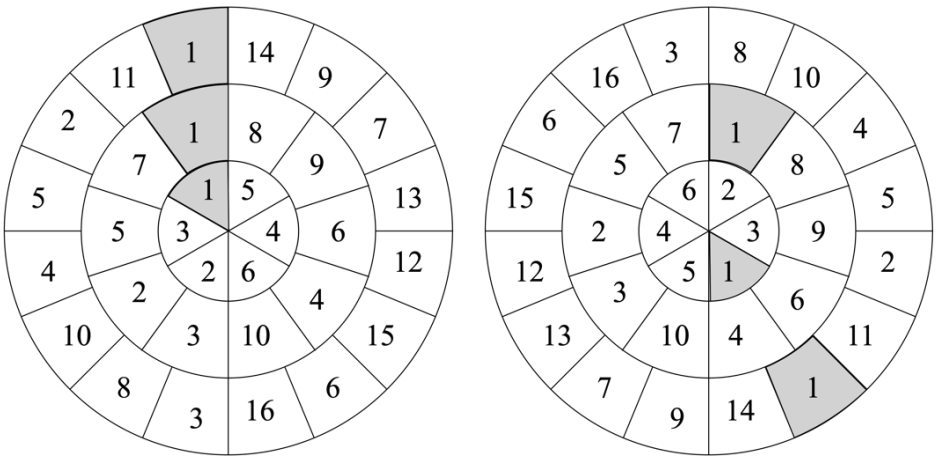


(a) (b)

Figure 4: An example of arranging the remainder sequence generated for a circular reflector.

Table 1: The primitive root $r$ of the prime number$p$ generated for the circular reflector and the remainder of its power.

| $n$ | $p$ | $r$ | index | | | | | | | | | | | | | | | | |
|---|---|---|---|---|---|---|---|---|---|---|---|---|---|---|---|---|---|---|---|
| | | (max.) | 1 | 2 | 3 | 4 | 5 | 6 | 7 | 8 | 9 | 10 | 11 | 12 | 13 | 14 | 15 | 16 | $\cdots$ |
| 1 | 7 | 5 | **5** | **4** | **6** | **2** | **3** | **1** | 5 | 4 | 6 | 2 | 3 | 1 | 5 | 4 | 6 | 2 | $\cdots$ |
| 2 | 11 | 8 | **8** | **9** | **6** | **4** | **10** | **3** | **2** | **5** | **7** | **1** | 8 | 9 | 6 | 4 | 10 | 3 | $\cdots$ |
| 3 | 17 | 14 | **14** | **9** | **7** | **13** | **12** | **15** | **6** | **16** | **3** | **8** | **10** | **4** | **5** | **2** | **11** | **1** | $\cdots$ |
| $\vdots$ | $\vdots$ | $\vdots$ | | | | | | | | | $\vdots$ | | | | | | | | |

eliminate the regularity of the radial repression as shown in Fig. 4(b).

Because of the discontinuity in the existence of prime numbers, some rings may have the same number of divisions as the one before. For example, for $n = 33$, a prime close to $(2 \times 33 - 1)\pi + 1 \fallingdotseq 205.20$ is $p = 211$, and even though for $n = 34$, the prime number close to $(2 \times 34 - 1)\pi + 1 \fallingdotseq 211.49$ is $p = 211$. Such case can be avoided by using different primitive roots. In this example, $r = 207$ and $r = 205$ can be used to generates completely different reminder sequences. Alternatively, the arrangement of the depressions can be shifted in the circumferential direction by one notch to prevent the same pattern of depressions on adjacent inner and outer surfaces.

## 3. REFLECTOR SUPPORTED BY MULTIPLE WAVELENGTHS

This section describes an applied reflector for multiple wavelengths. An example of the cross-section of a circular reflector with different wavelength in the center and periphery of the circle is is shown in Fig. 5. The proposed circular reflector differs from the rectangular reflector in that each ring can configure the reflectors of different wavelengths.

If the radius of the inner circular reflector corresponding to wavelength $\lambda_1$ is $r$, then the $n$th ring corresponding to wavelength $\lambda_2$ is a division by a prime number a prime number close to

$$p \fallingdotseq \pi\,(8r/\lambda_2 + 2n + 1) + 1. \tag{1}$$

## 4. DISTRIBUTION OF PRIME NUMBER AND REFLECTOR DESIGN

As the reflector size increases, a larger number of primes is required. On the other hand, it is known that the larger the number of primes, the wider the distribution interval.

As the reflector size increases, a larger number of primes is required. On the other hand, it is know that the larger the prime number, the wider the interval over which it is distributed. It is

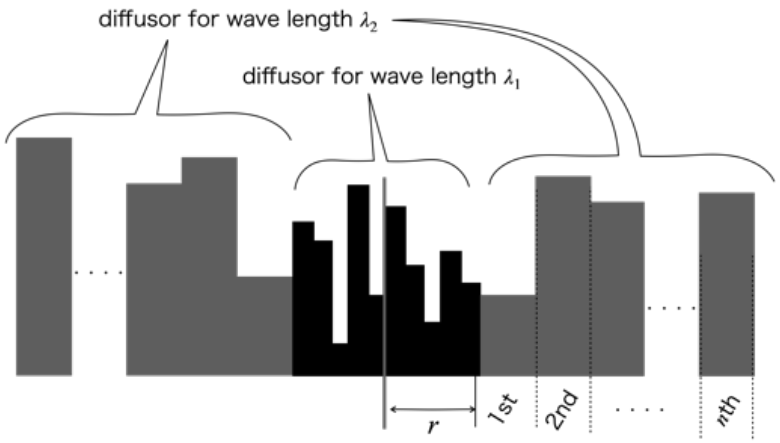


Figure 5: Cross sectional view of the reflector supported by multiple wavelengths.

necessary to prove that the relative error $(p_n - L_N(n))/p_n$ between the prime number $p_n$ and the target number of divisions $L_N(n)$ convergence. This section proves

$$\lim_{n\to\infty} \frac{p_n - L_N(n)}{p_n} = 0 \tag{2}$$

based on the Ingham's theorem [6].

Ingham's theorem, there exist sufficiently large positive constant $0 < c$ and $0 < \beta < 1$ such that $p_n - p_{n-1} < c p_{n-1^\beta}$. Let $p_n$ be the smallest prime greater than $L_N(n)$ and $p_{n-1}$ be the largest prime less than $L_N(n)$, then

$$0 < p_n - L_N(n) < p_n - p_{n-1}. \tag{3}$$

From Ingham's theorem,

$$0 < p_n - L_N(n) < p_n - p_{n-1} < c p_{n-1}^{\beta} \tag{4}$$

is obtained, and therefore

$$\begin{aligned} 0 < \frac{p_n - L_N(n)}{p_n} < \frac{c p_{n-1}^{\beta}}{p_n} &= c \left( \frac{p_{n-1}^{\beta}}{p_n} \right) \frac{1}{p_n^{1-\beta}} \\ &< \frac{c}{p_n^{1-\beta}} \end{aligned} \tag{5}$$

is valid. The right-hand side converges to 0 if $n \to \infty$, so

$$\lim_{n\to\infty} \frac{p_n - L_N(n)}{p_n} = 0 \tag{6}$$

holds.

## 5. PROTOTYPING USING 3D PRINTER

In this work, a prototype reflector for wavelength $\lambda = 136$mm (frequency is $f = 2.5$kHz) was manufactured using a 3D printer (Fig. 6(a)). The i-Fast manufactured by QIDI Technology (FDM: Fused Deposition Modeling) was used for the 3D printer, and PLA (Polylactic Acid) material manufactured by Mutoh Industries, Ltd. was used for the filament. The ring of the reflector is composed quintuple circle, and the diameter becomes 0.34m. Table 5 shows the prime number $p$ and the primitive roots $r$, and the remainder of the power of $r$ devided by $p$ used for the prototype. By arranging the remainder as shown in Fig. 6(b), projections proportional to the remainder value are arranged.

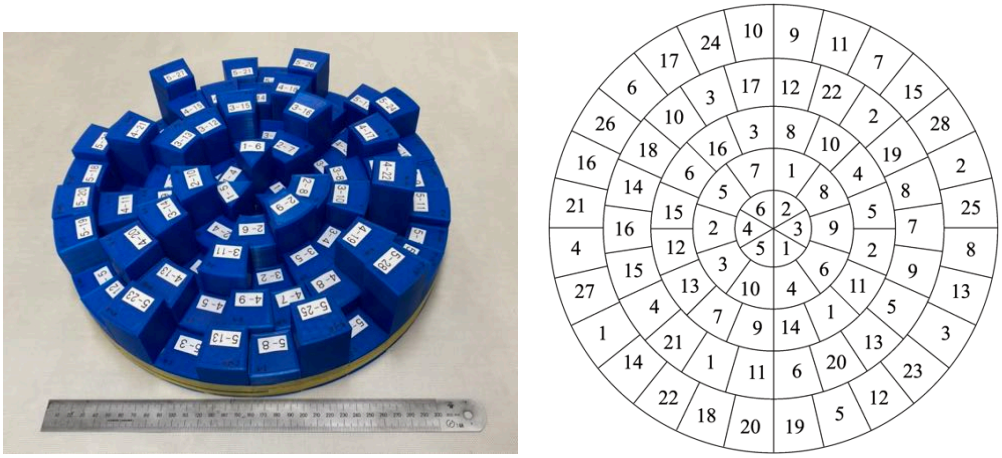

(a) (b)

Figure 6: Prototyped reflector using 3D printer (a) and the arrangement the remainder (b).

Table 2: The primitive root $r$ of the prime number $p$ using in the prototype reflector and the remainder of its power.

| $n$ | $p$ | $r$ | index | | | | | | | | | | | | | |
|---|---|---|---|---|---|---|---|---|---|---|---|---|---|---|---|---|
| | | | 10 | 11 | 12 | 13 | 14 | 15 | 16 | 17 | 18 | 19 | 20 | 21 | 22 | 23 |
| 1 | 7 | 5 | 2 | 3 | 1 | 5 | 4 | 6 | | | | | | | | |
| 2 | 11 | 8 | 1 | 8 | 9 | 6 | 4 | 10 | 3 | 2 | 5 | 7 | | | | |
| 3 | 17 | 14 | 8 | 10 | 4 | 5 | 2 | 11 | 1 | 14 | 9 | 7 | 13 | 12 | 15 | 6 |
| 4 | 23 | 21 | 12 | 22 | 2 | 19 | 8 | 7 | 9 | 5 | 13 | 20 | 6 | 11 | 1 | 21 |
| 5 | 29 | 27 | 9 | 11 | 7 | 15 | 28 | 2 | 25 | 8 | 13 | 3 | 23 | 12 | 5 | 19 |

| $n$ | $p$ | $r$ | index | | | | | | | | | | | | | |
|---|---|---|---|---|---|---|---|---|---|---|---|---|---|---|---|---|
| | | | 24 | 25 | 26 | 27 | 28 | 29 | 30 | 31 | 32 | 33 | 34 | 35 | 36 | 37 |
| 3 | 17 | 14 | 16 | 3 | | | | | | | | | | | | |
| 4 | 23 | 21 | 4 | 15 | 16 | 14 | 18 | 10 | 3 | 17 | | | | | | |
| 5 | 29 | 27 | 20 | 18 | 22 | 14 | 1 | 27 | 4 | 21 | 16 | 26 | 6 | 17 | 24 | 10 |

## 6. MEASUREMENT OF SCATTERING COEFFICIENT CONSIDERING EQUIVALENT SOUND ABSORPTION AREA

The scattering coefficient [7] is defined for a measure of the diffusion performance of a boundary surface, and the international standard ISO1749-1 [8] specifies the measurement method using an echoic room. Recently, a measurement method using a 1/4 scale model has been proposed [9]. The scattering coefficient is defined as the ratio of the reflected energy other than the specular reflection component to the total reflected energy, as in

$$S_c = \frac{\alpha_{spec} - \alpha_s}{1 - \alpha_s}, \tag{7}$$

using the sound absorption coefficient $\alpha_s$ of the sample and the sound absorption coefficient $\alpha_{spec}$ where only the specular reflection component is considered as the reflected energy. In the echoic room

method defined by international standards, the sound absorption coefficient of each is determined by

$$\alpha_s = 24\ln 10 \frac{V}{S}\left(\frac{1}{c_2 T_2} - \frac{1}{c_1 T_1}\right) \tag{8}$$

$$\alpha_{spec} = 24\ln 10 \frac{V}{S}\left(\frac{1}{c_4 T_4} - \frac{1}{c_3 T_3}\right), \tag{9}$$

where $V$ is the volume of the echoic room, $S$ is the wall area of the echoic room, and $T_i$ is the reverberation time measured using the conditions shown in Table 6. Also, $c_i$ is the sound speed at each measurement. However, the volume of the echoic room is sufficiently small that the sound absorption coefficient of the air can be neglected, or the sound absorption coefficient of the air must remain constant during the experiment.

However, the conventional echoic room method does not considered account the ratio of the area of the sample to the total wall area of the echoic room. In the case of an experiment using a scale model of echoic room, if the length is reduced by $1/10$, the wall area is reduced by $1/100$ and the room volume is reduced by $1/1000$, resulting in a reverberation time of about $1/10$. Therefore the problem of changing the obtained scattering coefficient is concerned.

Table 3: Measurement conditions of reverberation times for scattering coefficient in reverberant chamber.

| Reverberation Time | Sound speed | Sample | Turntable |
|---|---|---|---|
| $T_1$ | $c_1$ | not present | not rotating |
| $T_2$ | $c_2$ | present | not rotating |
| $T_3$ | $c_3$ | not present | rotating |
| $T_4$ | $c_4$ | present | rotating |

On the other hand, Eying's reverberation time equation for a echoic room with room volume $V$, wall area $S_0$, and wall sound absorption coefficient $\alpha_0$, and a sample with area $S_s$ and sound absorption coefficient $\alpha_s$ can be expressed as

$$T_R \simeq \frac{(24\ln 10)V}{(S_0\,\alpha_0 + S_s\,\alpha_s)\,c}, \tag{10}$$

using the equivalent sound absorption area $S_0\,\alpha_0 + S_s\,\alpha_x$. Provided that, the sound absorption coefficient $\alpha$ should be small enough to approximate $-\ln(1-\alpha) \simeq \alpha$. Therefore, the sound absorption coefficient of the sample can be expressed as

$$\alpha_s \simeq \frac{(24\ln 10)V}{T_R\,c\,S_s} - \frac{S_0}{S_s}\,\alpha_0. \tag{11}$$

Based on this relationship, the sound absorption coefficient of the sample $\alpha_s$ and the sound absorption coefficient $\alpha_{spec}$, where only the specular reflection component is considered as reflected energy, can be obtained as

$$\alpha_s = \frac{(24\ln 10)V}{T_2\,c_2\,S_x} - \frac{(S_0 - S_x)}{S_x}\,\alpha_0 \tag{12}$$

$$\alpha_{spec} = \frac{(24\ln 10)V}{T_4\,c_4\,S_x} - \frac{(S_0 - S_x)}{S_x}\,\alpha_0 \tag{13}$$

using the reverberation time in Table 6. The $\alpha_0$ can be obtained from

$$\alpha_0 = \frac{(24\ln 10)V}{T_1\,c_1\,S_0}. \tag{14}$$

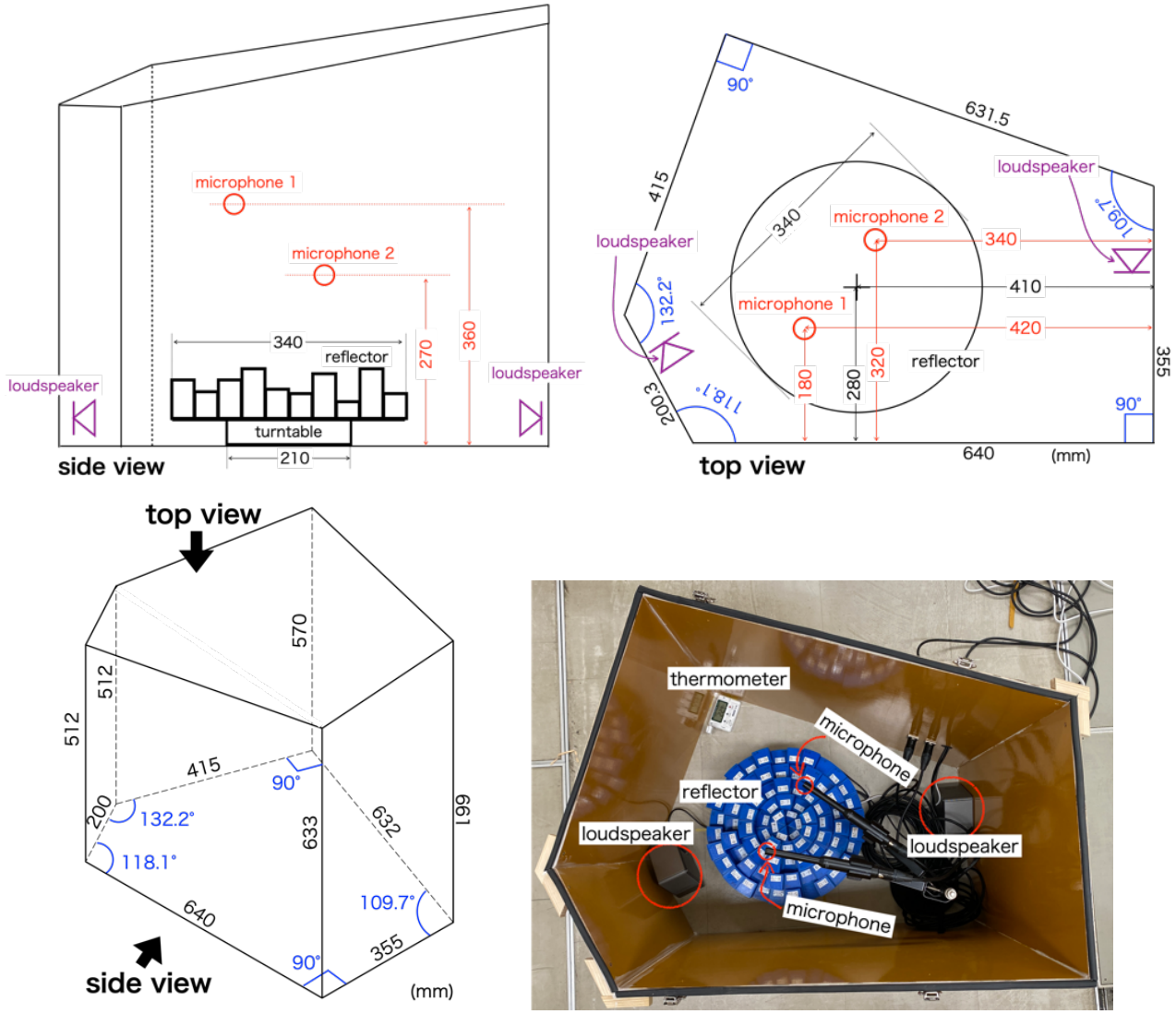


Figure 7: Irregularly shaped reverberation box and arrangement of equipment in the experiment

## 7. MEASUREMENT OF SCATTERING COEFFICIENT USING SCALE MODEL OF ECHOIC ROOM

In this work, it is attempted to measure the scattering coefficient of a prototyped reflector using a model echoic room. A model echoic room with a room volume of 0.186m$^3$ and a wall area of 1.948m$^2$ was used in the experiment. The turntable that rotates the reflector has a diameter of 21cm and a hight of 5cm and rotates once in 66 seconds. An acrylic plate with a size equal to the diameter of the prototype reflector, 34cm was pasted on the rotating plate. In all experiments, the turntable was always set up for the purpose of matching conditions. The impulse response required to calculate the reverberation time was measured by the TSP method. Recording and played back were performed at sampling frequencies of 48kHz and a quantization of 24bits. The TSP length was set to $2^{14}$ samples (341.3ms), and 79616 points of zero were inserted after the TSP signal to make a 2 second signal. This signal was replayed 66 times and synchronously added. The sound velocity at each measurement was calculated from the average of the temperatures at the beginning and end of the measurement. An omnidirectional microphone (Audix, TR40A) was used for measurements. Fig. 7 shows the dimensions of the model echoic room and the layout of the equipment.

The observed impulse response was divided into 1/3 octave frequency bands, and the reverberation time $T_{10}$ was calculated for each frequency band. Fig. 8 shows the results of the scattering coefficient analysis. The results of scattering coefficient analyzed using Equation (12) (13), taking into account the equivalent sound absorption area, are shown in ∘, and the results using

the conventional method, Equation (8) (9), are shown in △. The conventional method does not show any significant effect of reflectors. On the other hand, the results considering the equivalent sound absorption area show that the scattering coefficient increases from a frequency band one octave lower than 2.5kHz, the frequency range of the prototype reflector, and that the diffusion performance increases.

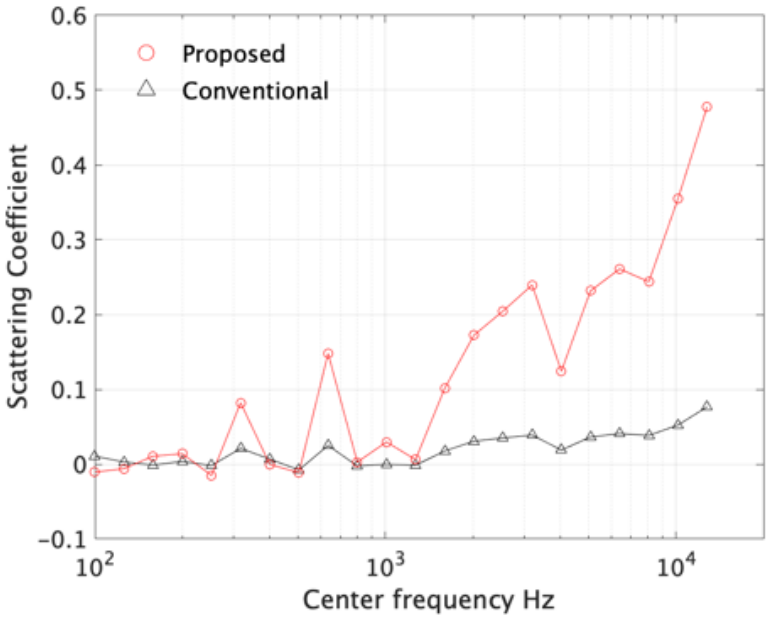


Figure 8: Scattering coefficient

## 8. CONCLUSION

This report proposes a circular reflector based on primitive roots. The proposed reflector generation The proposed reflector generation method makes it possible to change the design from rectangular to circular. Reflectors based on number theory are designed to target specific frequency band. On the other hand, the circular reflectors can mix reflectors corresponding to multiple frequency bands in one reflector. The proposed method requires a larger number of primes as the reflectors become larger, whereas the larger the number of primes, the wider the spacing of the distribution. In this work, it was proved based on Ingham's theorem, that the relative error between primes and divisions converges as the reflector size increases and the number of divisions increases.

In this work, a prototype of the proposed reflector was fabricated using a 3D printer. The scattering coefficient was then measured using a model echoic room. The measurement of scattering coefficient specified in ISO does not take into account the area of the sample in the wall area of the echoic room. Therefore, in this experiment using a scaled model of a echoic room, it was attempted to analyze the scattering coefficient by considering the equivalent sound absorption area. As a result, it was confirmed that the scattering coefficient increased from a frequency band about one octave lower than that of the prototype reflector and tha sound waves were diffused.

## REFERENCES

1. M. R. Schroeder, D. Gottlob, and K. F. Siebrasse. Comparative study of european concert halls. *J. Acoust. Soc. Am.*, 56:1195—1201, 1974.
2. M. R. Schroeder. Binaural dissimilarity and optimum ceilings for concert halls: More lateral sound diffusion. *J. Acoust. Soc. Am.*, 65:958—963, 1979.
3. M. R. Schroeder. *Number Theory in Science and Communication*. Springer, 1984.

4. A. Nowoświat, M. Olechowska, and M. Marchacz. The effect of acoustical remedies changing the reverberation time for different frequencies in a dome used for worship: A case study. *Applied Acoustics*, 160:1–10, 2020.
5. N. Kanazawa, Y. Takahashi, and I. Makino. Circular acoustic reflector based on primitive roots. In *Proc. Autumn Meet. Acoust. Soc. Jpn.*, pages 815–816, Hokkaido, Japan, September 2022.
6. A. E. Ingham. On the difference between consecutive primes. *J. Math. Oxford Series*, 8(1):255–266, 1937.
7. M. Vorländer and E. Mommertz. Definition and measurement of random-incidence scattering coefficients. *Applied Acoustics*, 60:187–199, 2000.
8. Acoustics - sound-scattering properties of surfaces, part 1: Measurement of the random-incidence scattering coefficient in a reverberation room. ISO 17497-1, 2004.
9. Y. Tsuchiya, H. Lee, and T. Sakuma. Scale model measurment of the scattering coefficients of rib/block structure walls. *AIJ J. Technol. Des. (in Japanese and English abstract)*, 19(41):175–178, 2013.